Pergamon

Int. J. Solids Structures Vol. 34, No. 21, pp. 2669–2684, 1997

0020–7683/97 $17.00 + .00

PII: S0020–7683(96)00163–1

IMPACT RESPONSE OF COMPOSITE CYLINDERS

S. A. MATEMILOLA and W. J. STRONGE
Cambridge University Engineering Department, Trumpington Street,
Cambridge CB2 1PZ, U.K.

(*Received* 24 *April* 1996; *in revised form* 25 *July* 1996)

Abstract—An analytical solution has been developed for the impact response of a simply supported anisotropic composite cylinder. The contact force was obtained from the compatibility condition between the elastic impactor and the cylinder, with a modified Hertzian law. The Hertzian contact force term introduces a slight nonlinearity in the variation of contact force amplitude with velocity of impact. The present analysis also incorporates the terms that arise in the expressions for stress resultants and stress couples due to the trapezoidal shape of an elemental section of a shell. These trapezoidal terms can cause significant effects on the strain response of thick shell elements if the composite layup is non-symmetric. © 1997 Elsevier Science Ltd.

1. INTRODUCTION

Composite materials are increasingly finding application in shell structures such as pressure vessels, pipe lines, rocket motor casing, to name a few. Despite the fact that most composite structures are rarely completely flat in practice, most of the research focus has been on plate and beam structures, while relatively little research has been carried out on composite shell structures. Nevertheless, most of the methods that have been applied in the analysis of flat plates are also applicable for shell structures.

Some of the recent studies on dynamics of non-planar composite structures include that by Bert and Birman (1988), who conducted a parametric study of the dynamic instability of simply supported circular cylindrical shells using a first order shear deformable theory. Ramkumar and Thakar (1987), studied the impact response of curved laminated plates, using Donnel's approximations for thin shells. They represented the load and the radial displacements by Fourier series expansions, and calculated the deflections and the back surface strains due to a known linear force history. In a similar study conducted by Christoforou and Swanson (1990), the authors neglected the local contact deformation in deriving the equilibrium equation between the striker and the cylinder. The resulting integral equation was then solved using a combination of Laplace transform technique and the Cauchy residue theorem. Chandrashekhara and Schroeder (1995) studied the nonlinear impact response of cylindrical and doubly curved shells using a finite element technique. Their analysis was based on Sander's shell theory, and included shear deformation effects.

In the present study, the impact response of an orthotropic cylinder is analysed. By considering compatibility of displacements between the impactor and the cylinder, an expression is obtained from which the contact force history is calculated using Muller's root search method. In the analysis of shell structures most authors usually consider as negligible, terms that arise due to the trapezoidal shape of the cross-section of an element of the shell. The inconsistency that this assumption introduces in the formulation of the governing equations was first highlighted by Flügge (1973). Although, in most cases, especially for thin shells, the strains calculated based on such an analysis are not significantly affected, for thick shells this can lead to significant errors in the calculated moments and forces.

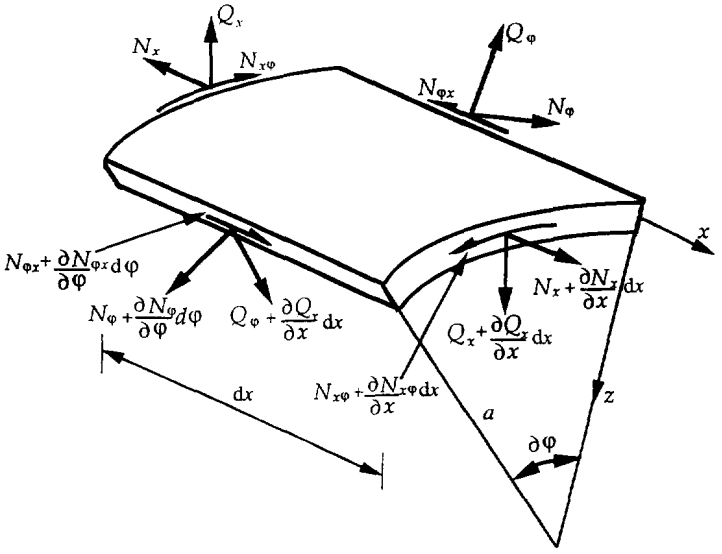

Fig. 1. An elemental section of cylinder and coordinate system.

2. GOVERNING EQUATIONS

The equations of motion for an elemental section of a circular cylindrical shell (Fig. 1) with mass density per unit length ρ, radius a, and thickness h are, after elimination of transverse shear forces:

$$\frac{\partial N_x}{\partial x}+\frac{1}{a}\frac{\partial N_{\varphi x}}{\partial x}=\rho h\frac{\partial^2 u}{\partial t^2}$$

$$\frac{1}{a}\frac{\partial N_\varphi}{\partial \varphi}+\frac{\partial N_{x\varphi}}{\partial x}-\frac{1}{a}\frac{\partial M_\varphi}{\partial \varphi}+\frac{1}{a^2}\frac{\partial M_{x\varphi}}{\partial x}=\rho h\frac{\partial^2 v}{\partial t^2}$$

$$\frac{1}{a^2}\frac{\partial^2 M_\varphi}{\partial \varphi^2}-\frac{1}{a}\frac{\partial^2 M_{x\varphi}}{\partial x\partial \varphi}+\frac{\partial^2 M_{\varphi x}}{\partial x\partial \varphi}+\frac{\partial^2 M_x}{\partial x^2}+\frac{1}{a}N_\varphi+q=\rho h\frac{\partial^2 w}{\partial t^2} \tag{1}$$

where M_x, M_φ, $M_{x\varphi}$, $M_{\varphi x}$ are stress couples, N_x, N_φ, $N_{x\varphi}$ are stress resultants, and u, v, w are the displacements along the axis of the cylinder x, the hoop direction φ, and the radial direction z, respectively. The stress resultants and stress couples on an element of the cylindrical shell are related to the stress components as

$$N_x=\int_{-h/2}^{h/2}\sigma_x\left(1-\frac{z}{a}\right)dz, \qquad N_\varphi=\int_{-h/2}^{h/2}\sigma_\varphi\,dz,$$

$$N_{x\varphi}=\int_{-h/2}^{h/2}\tau_{x\varphi}\left(1-\frac{z}{a}\right)dz, \qquad N_{\varphi x}=\int_{-h/2}^{h/2}\tau_{\varphi x}\,dz,$$

$$M_x=\int_{-h/2}^{h/2}\sigma_x\left(1-\frac{z}{a}\right)z\,dz, \qquad M_\varphi=\int_{-h/2}^{h/2}\sigma_\varphi\,dz,$$

$$M_{x\varphi}=\int_{-h/2}^{h/2}\tau_{x\varphi}\left(1-\frac{z}{a}\right)z\,dz, \qquad M_{\varphi x}=\int_{-h/2}^{h/2}\tau_{\varphi x}\,zdz. \tag{2}$$

Whereas the shear stresses $\tau_{x\varphi}$, $\tau_{\varphi x}$ are equal, $\tau_{x\varphi}=\tau_{\varphi x}$, the stress couples and the stress resultants are unequal, $M_{x\varphi}\neq M_{\varphi x}$ and $N_{x\varphi}\neq N_{\varphi x}$, due to the term z/a which arises due to the trapezoidal shape of the cross-section of an element of the shell. This is because for an element of the cylinder, two opposite sides on the cylindrical section are trapezoids, and

their centroids lie slightly outside the middle surface (Flügge, 1973). The extra term that accounts for this effect of shell curvature is usually small, and may be negligible in the case of a thin shell. However, for an accurate formulation of the elasticity solution for a shell it is necessary to retain this difference. For example, by considering moments about a radius of the cylinder, an equilibrium condition may be written,

$$N_{x\varphi} - N_{\varphi x} + \frac{1}{a} M_{\varphi x} = 0. \tag{3}$$

This condition will no longer be satisfied if $N_{x\varphi} = N_{\varphi x}$, since in general, $M_{\varphi x} \neq 0$.

The stress resultants and stress couples may be expressed in terms of the stiffness matrices for the laminate as,

$$\begin{Bmatrix} N_x \\ N_\varphi \\ N_{x\varphi} \\ N_{\varphi x} \end{Bmatrix} = \begin{bmatrix} A_{11} - B_{11}/a & A_{12} - B_{12}/a & A_{16} - B_{16}/a \\ A_{12} & A_{22} & A_{26} \\ A_{16} - B_{16}/a & A_{26} - B_{26}/a & A_{66} - B_{66}/a \\ A_{16} & A_{26} & A_{66} \end{bmatrix} \begin{Bmatrix} \varepsilon_x^0 \\ \varepsilon_\varphi^0 \\ \gamma_{x\varphi}^0 \end{Bmatrix} + \begin{bmatrix} B_{11} - D_{11}/a & B_{12} - D_{12}/a & B_{16} - D_{16}/a \\ B_{12} & B_{22} & B_{26} \\ B_{16} - D_{16}/a & B_{26} - D_{26}/a & B_{66} - D_{66}/a \\ B_{16} & B_{26} & B_{66} \end{bmatrix} \begin{Bmatrix} \kappa_x \\ \kappa_\varphi \\ \kappa_{x\varphi} \end{Bmatrix} \tag{4}$$

and

$$\begin{Bmatrix} M_x \\ M_\varphi \\ M_{x\varphi} \\ M_{\varphi x} \end{Bmatrix} = \begin{bmatrix} B_{11} - D_{11}/a & B_{12} - D_{12}/a & B_{16} - D_{16}/a \\ B_{12} & B_{22} & B_{26} \\ B_{16} - D_{16}/a & B_{26} - D_{26}/a & B_{66} - D_{66}/a \\ B_{16} & B_{26} & B_{66} \end{bmatrix} \begin{Bmatrix} \varepsilon_x^0 \\ \varepsilon_\varphi^0 \\ \gamma_{x\varphi}^0 \end{Bmatrix} + \begin{bmatrix} D_{11} - L_{11}/a & D_{12} - L_{12}/a & D_{16} - L_{16}/a \\ D_{12} & D_{22} & D_{26} \\ D_{16} - L_{16}/a & D_{26} - L_{26}/a & D_{66} - L_{66}/a \\ D_{16} & D_{26} & D_{66} \end{bmatrix} \begin{Bmatrix} \kappa_x \\ \kappa_\varphi \\ \kappa_{x\varphi} \end{Bmatrix} \tag{5}$$

where A_{ij}, B_{ij}, D_{ij} and L_{ij} $(i,j = 1,2,6)$ are elements of stiffness matrices, and are defined in terms of the plane stress reduced elastic stiffness Q as

$$(A_{ij}, B_{ij}, D_{ij}, L_{ij}) = \int_{-h/2}^{h/2} (1, z, z^2, z^3) \bar{Q}_{ij} \, dz. \tag{6}$$

The reduced elastic stiffness matrix, $\bar{Q}_{ij}$ relates the lamina elastic stresses and strains in global coordinates (Agarwal and Broutman, 1990);

$$\begin{Bmatrix} \sigma_x \\ \sigma_\varphi \\ \tau_{x\varphi} \end{Bmatrix} = \begin{bmatrix} \bar{Q}_{11} & \bar{Q}_{12} & \bar{Q}_{16} \\ \bar{Q}_{12} & \bar{Q}_{22} & \bar{Q}_{26} \\ \bar{Q}_{16} & \bar{Q}_{26} & \bar{Q}_{66} \end{bmatrix} \begin{Bmatrix} \varepsilon_x \\ \varepsilon_\varphi \\ \gamma_{x\varphi} \end{Bmatrix}. \tag{7}$$

The midplane strains ε_x^0, ε_φ^0, $\gamma_{x\varphi}^0$ and curvatures κ_x, κ_φ, and the rotation $\kappa_{x\varphi}$, in the cylinder are (Timoshenko and Woinowski-Krieger, 1970),

$$\varepsilon_x^0 = \frac{\partial u}{\partial x}, \qquad \kappa_x = \frac{\partial^2 w}{\partial x^2},$$

$$\varepsilon_\varphi^0 = \frac{1}{a}\left(\frac{\partial v}{\partial \varphi} - w\right), \quad \kappa_\varphi = \frac{1}{a^2}\left(\frac{\partial^2 w}{\partial \varphi^2} + \frac{\partial v}{\partial \varphi}\right),$$

$$\gamma_{x\varphi}^0 = \frac{1}{a}\frac{\partial u}{\partial \varphi} + \frac{\partial v}{\partial x}, \quad \kappa_{x\varphi} = \frac{1}{a}\frac{\partial^2 w}{\partial x \partial \varphi} + \frac{1}{a}\frac{\partial v}{\partial x}, \tag{8}$$

and are related to the strain distributions in the cylinder,

$$\varepsilon_x = \varepsilon_x^0 - z\kappa_x,$$

$$\varepsilon_\varphi = \varepsilon_\varphi^0 - z\kappa_\varphi,$$

$$\gamma_{x\varphi} = \gamma_{x\varphi}^0 - z\kappa_{x\varphi}. \tag{9}$$

The equations of motion can be further simplified by considering a specially orthotropic material with elastic stiffness matrix coefficients $A_{16} = A_{26} = B_{16} = B_{26} = D_{16} = D_{26} = L_{16} = L_{26} = 0$. Materials whose stiffness matrix properties satisfy this condition include composite laminates composed wholly of 0° and 90° fibre orientations. Using the notations;

$$A_{ij}^* = A_{ij} - \frac{B_{ij}}{a} \quad (i,j = 1,2,6),$$

$$B_{ij}^* = B_{ij} - \frac{D_{ij}}{a}$$

$$D_{ij}^* = D_{ij} - \frac{L_{ij}}{a} \tag{10}$$

the equations of motion in terms of strains take the form

$$A_{11}^*\frac{\partial \varepsilon_x^0}{\partial x} + A_{12}^*\frac{\partial \varepsilon_\varphi^0}{\partial x} - B_{11}^*\frac{\partial \kappa_x}{\partial x} - B_{12}^*\frac{\partial \kappa_\varphi}{\partial x} + \frac{1}{a}\left(A_{66}\frac{\partial \gamma_{x\varphi}^0}{\partial \varphi} - B_{66}\frac{\partial \kappa_{x\varphi}}{\partial \varphi}\right) = \rho h\frac{\partial^2 u}{\partial t^2}$$

$$\frac{1}{a}\left(A_{12}\frac{\partial \varepsilon_x^0}{\partial \varphi} + A_{22}\frac{\partial \varepsilon_\varphi^0}{\partial \varphi} - B_{12}\frac{\partial \kappa_x}{\partial \varphi} - B_{22}\frac{\partial \kappa_\varphi}{\partial \varphi}\right) + A_{66}^*\frac{\partial \varepsilon_{x\varphi}^0}{\partial \varphi} - B_{66}^*\frac{\partial \kappa_{x\varphi}}{\partial \varphi}$$

$$-\frac{1}{a^2}\left(B_{12}\frac{\partial \varepsilon_x^0}{\partial \varphi} + B_{22}\frac{\partial \varepsilon_\varphi^0}{\partial \varphi} - D_{12}\frac{\partial \kappa_x}{\partial \varphi} - D_{22}\frac{\partial \kappa_\varphi}{\partial \varphi}\right) + \frac{1}{a}\left(B_{66}^*\frac{\partial \gamma_{x\varphi}^0}{\partial x} - D_{66}^*\frac{\partial \kappa_x}{\partial x}\right) = \rho h\frac{\partial^2 v}{\partial t^2}$$

$$\frac{1}{a^2}\left(B_{12}\frac{\partial^2 \varepsilon_x^0}{\partial \varphi^2} + B_{22}\frac{\partial^2 \varepsilon_\varphi^0}{\partial \varphi^2} - D_{12}\frac{\partial^2 \kappa_x}{\partial \varphi^2} - D_{22}\frac{\partial^2 \kappa_\varphi}{\partial \varphi^2}\right)$$

$$+\frac{1}{a}\left((B_{66} + B_{66}^*)\frac{\partial^2 \gamma_{x\varphi}^0}{\partial x \partial \varphi} - (D_{66} - D_{66}^*)\frac{\partial^2 \kappa_{x\varphi}}{\partial x \partial \varphi}\right) + B_{11}^*\frac{\partial^2 \varepsilon_x^0}{\partial x^2} + B_{12}^*\frac{\partial^2 \varepsilon_\varphi^0}{\partial x^2}$$

$$-D_{11}^*\frac{\partial^2 \kappa_x}{\partial x^2} - D_{12}^*\frac{\partial^2 \kappa_\varphi}{\partial x^2} - \frac{1}{a}(A_{12}\varepsilon_x^0 + A_{22}\varepsilon_\varphi^0 - B_{12}\kappa_x - B_{22}\kappa_\varphi) + q = \rho h\frac{\partial^2 w}{\partial t^2}. \tag{11}$$

3. METHOD OF SOLUTION

For a cylinder with simply supported ends, a closed form solution that also satisfies the conditions of symmetry of deformation is obtained by representing displacement components in terms of a double series (Flügge, 1973),

$$u = \sum_{m=0}^{\infty}\sum_{n=1}^{\infty} U_{mn}(t)\cos n\varphi \cos \lambda x,$$

$$v = \sum_{m=1}^{\infty}\sum_{n=1}^{\infty} V_{mn}(t)\sin n\varphi \sin \lambda x,$$

$$w = \sum_{m=1}^{\infty}\sum_{n=0}^{\infty} W_{mn}(t)\cos n\varphi \sin \lambda x, \tag{12}$$

and the applied load, q, is given by

$$q = \sum_{m=1}^{\infty}\sum_{n=0}^{\infty} Q_{mn}(t)\cos n\varphi \sin \lambda x \tag{13}$$

where λ is related to the length of the cylinder l, and the axial mode number m,

$$\lambda = \frac{m\pi}{l}. \tag{14}$$

In their study on dynamic stability of cylindrical shells, Bert and Birman (1988) have shown that the effects of in-plane inertia are negligible. Based on this assumption the governing equation for the cylinder in terms of the displacement components may be obtained by writing the strain components in terms of the displacements components eqn (8), and using eqn (12) in the governing eqns (11),

$$\begin{bmatrix} C_{11} & C_{12} & C_{13} \\ C_{21} & C_{22} & C_{23} \\ C_{31} & C_{32} & C_{33} \end{bmatrix} \begin{Bmatrix} U_{mn} \\ V_{mn} \\ W_{mn} \end{Bmatrix} = \begin{Bmatrix} 0 \\ 0 \\ \rho h \dfrac{\partial^2 W}{\partial t^2} - Q_{mn} \end{Bmatrix} \tag{15}$$

where the coefficients C_{ij} $(i,j = 1,2,3)$ are,

$$C_{11} = -\left\{\lambda^2 A_{11}^* + \frac{n^2}{a^2} A_{66}\right\}$$

$$C_{12} = \frac{\lambda n}{a}\left(A_{12}^* + A_{66} - \frac{B_{12}^*}{a} - \frac{B_{66}}{a}\right)$$

$$C_{13} = -\frac{\lambda}{a} A_{12}^* + \lambda^3 B_{11}^* + \frac{n^2\lambda}{a^2}(B_{12}^* + B_{66})$$

$$C_{21} = \frac{\lambda n}{a}\left(A_{12} + A_{66}^* - \frac{B_{12}^*}{a} - \frac{B_{66}}{a}\right)$$

$$C_{22} = -\left\{\frac{n^2}{a^2}\left(A_{22} - 2\frac{B_{22}}{a} - \frac{D_{22}}{a^2}\right) + \lambda^2\left(A_{66}^* + \frac{B_{66}}{a} - \frac{B_{66}^*}{a} - \frac{D_{66}^*}{a^2}\right)\right\}$$

$$C_{23} = \frac{n}{a}\left\{\frac{A_{22}}{a} - \frac{(n^2+1)}{a^2}B_{22} + \frac{n^2}{a^3}D_{22} + \lambda^2\left(B^*_{66} - B_{12} + \frac{D_{12}}{a} + \frac{D^*_{66}}{a}\right)\right\}$$

$$C_{31} = -\frac{\lambda}{a}A_{12} + \lambda^3 B^*_{11} + \frac{n^2\lambda}{a^2}(B_{12} + B_{66} - B'_{66})$$

$$C_{32} = \left\{\frac{n}{a^2}A_{22} - \frac{n(n^2+1)}{a^3}B_{22} + \frac{n^3}{a^4}D_{22} + \frac{\lambda^2 n}{a}\left(B^*_{66} - B^*_{12} - B_{66} + \frac{D_{12} + D_{66} - D^*_{66}}{a}\right)\right\}$$

$$C_{33} = -\left\{\frac{A_{22}}{a^2} - \frac{2n^2}{a^3}B_{22} - \frac{\lambda^2}{a}(B_{12} + B^*_{12}) + \lambda^4 D^*_{11} + \frac{n^4}{a^4}D_{22} + \frac{\lambda^2 n^2}{a^2}(D_{12} + D^*_{12} + D_{66} - D^*_{66})\right\}. \tag{16}$$

Equation (15) can be reduced to a single equation,

$$\frac{\partial^2 W_{mn}}{\partial t^2} + \omega^2_{mn} W_{mn} = \frac{Q_{mn}}{\rho h} \tag{17}$$

where the natural frequencies of the cylinder are given by

$$\omega_{mn} = \sqrt{(C_{31}K_a + C_{32}K_b - C_{33})/\rho h} \tag{18}$$

and

$$K_a = \frac{C_{13}C_{22} - C_{12}C_{23}}{C_{11}C_{22} - C_{12}C_{21}},$$

$$K_b = \frac{C_{13}C_{21} - C_{11}C_{23}}{C_{11}C_{22} - C_{12}C_{21}}. \tag{19}$$

The contact load is assumed to be uniform and is distributed as a double half-sine pulse over a small rectangular area, with length χ and subtending an angle β in the hoop direction. The centre of the loaded region is located at ξ, ζ, along the x and the φ coordinates of the cylinder, respectively. The dynamic component of the applied load has the form

$$Q_{mn}(t) = \frac{16F(t)}{\pi^2 nm\chi\beta a}\sin\frac{m\pi}{l}\xi\cos n\zeta\sin\frac{m\pi}{l}\frac{\chi}{2}\sin n\frac{\beta}{2} \tag{20}$$

where $F(t)$ is the impact force.

The initial conditions for the problem are zero initial displacement and velocity, and thus, the solution of (17) is given by the convolution integral

$$W_{mn}(t) = \frac{1}{\rho h\omega_{mn}}\int_0^t Q_{mn}(t)\sin\omega_{mn}(t-\tau)\,d\tau. \tag{21}$$

4. IMPACT LOADING

The contact force $F(t)$ between the striker and the cylinder is obtained by considering the approach $\alpha(t)$ between the two bodies (Lee, 1940; Goldsmith, 1960),

$$\alpha(t) = v_0 t - \frac{1}{m}\int_0^t F(t)(t-\tau)\,\mathrm{d}\tau - w(t) \tag{22}$$

where v_0 is the velocity of collision and m is the mass of the striker. The transverse displacement component $w(t)$ is obtained by substituting eqn (21) into the last of (12). The approach $\alpha(t)$ is given by Hertz contact law,

$$\alpha(t) = \left(\frac{F(t)}{k}\right)^{2/3} \tag{23}$$

where the contact stiffness k, is related to the elastic and the geometric properties of the striker and the target as (Chandrashekhara and Schroeder, 1995),

$$k = \frac{4}{3}\frac{1}{3(1-v_s^2)/E_s + (1-v_{zt}^2)/E_z}\sqrt{\frac{R_c R_s}{R_c + R_s/2}}. \tag{24}$$

In the above equation, v is Poisson's ratio, E is Young's modulus and R is surface radius. The subscripts s and c refer to the striker and the cylinder, respectively, and z is the through-thickness direction. Detailed studies on the contact stiffness for carbon fibre composite materials have been carried out by Yang and Sun (1982), as well as by Tan and Sun (1985). Substituting eqns (21) and (23) into (22) yields

$$\left(\frac{F(t)}{k}\right)^{2/3} = v_0 \mathrm{t} - \frac{1}{\mathrm{m}}\int_0^t \mathrm{F(t)(t-\tau)d\tau} - \sum_m^\infty\sum_n^\infty \rho h \frac{1}{\omega_{mn}}\int_0^t Q_{mn}(\tau)\sin\omega_{mn}(t-\tau)\mathrm{d}\tau. \tag{25}$$

By subdividing the contact duration into j time intervals with small time increments Δt, and performing the integration over each time step, eqn (25) may be written as

$$\left(\frac{F(t)}{k}\right)^{2/3} = v_0 j\Delta t - \frac{1}{m}\sum_{i=1}^{j} F_i \Delta t^2\left(j-1+\frac{1}{2}\right) - \sum_m^\infty\sum_n^\infty \frac{P_{mn}}{\rho h\omega_{mn}^2}\sum_{i=1}^{j} F_i\{\cos\omega_{mn}(j-i)\Delta t - \cos\omega_{mn}(j-i+1)\Delta t\} \tag{26}$$

where

$$P_{mn} = \frac{8}{\pi^2 nm\alpha\beta a}\sin\frac{m\pi}{l}\xi\cos n\zeta\sin\frac{m\pi}{2l}\alpha\sin\frac{n}{2}\beta. \tag{27}$$

In the numerical examples that follow, for good accuracy the contact duration was divided into a total of at least $j = 400$ time intervals, so as to give at least 150 time steps in the period up to the time of peak force (Qian and Swanson, 1990). The contact force $F(t)$ (taken as constant over each time increment) at the end of each time duration was then calculated from eqn (26), using Muller's root search method (Gerald and Wheatley, 1989). This contact force history was then substituted into eqn (21) to obtain the transverse displacement response, and the displacement components substituted into eqn (9) by using (8) to obtain the strain components.

5. RESULTS AND DISCUSSION

The solution procedure outlines above is verified by comparing the impact force response computed from eqn (26) with experimental results obtained by Gong (1995, 1996).

Open ended filament wound glass fibre composite cylinders were used in this experiment (their properties are listed in Table 1). In order to simulate simply supported boundaries, the test cylinder was supported by wooden cradles that were located 280 mm apart. Thin wires were then wrapped round the cylinder at the supported sections, and tied to the cradles. Because of the large ratio of radius to wall thickness for this cylinder $a/h \approx 47$, the natural frequency initially decreases, and later begins to slowly increase with increase in circumferential wave number. This is because for such thin walled cylinder, for a fixed axial wave number there is a decrease in the membrane strain energy and an increase in the bending strain energy as the circumferential wave number increases (Flügge, 1973; Bert and Kumar, 1982). Thus, in order to achieve proper convergence, at least 69 modal terms were used in all the examples considered.

Figures 2(a), (b) and (c) show the force history for impact on this composite shell at 1 ms^{-1}, 3 ms^{-1} and 5 ms^{-1}, respectively. The figures show that whereas the contact period did not change appreciably for all three values of impact velocity, the peak force varies almost linearly with the velocity of impact. The hoop strain response (shown in Fig. 3(a)) and the axial strain response (shown in Fig. 3(b)) on the distal surface of the shell, the impact point, both show an almost linear variation with impact velocity. Figure 4 shows the effect of the ratio of hoop to axial Young's moduli E_1/E_2 on the contact force and strains due to a 0.075 kg mass colliding at 1 ms^{-1} against a hoop wound composite cylinder (the axial Young's modulus was kept constant while the hoop Young's modulus was varied). As expected, the contact force increased with increase in hoop stiffness of the composite cylinder. As the Young's modulus was increased in the hoop direction, both the axial strain as well as the hoop strain decreased. However, there was a greater reduction in hoop strain due to the increase in stiffness in that direction.

For a 2.3 mm thick hoop wound composite cylinder whose properties are given in Table 1, the strain responses at different positions away from the region of impact (measured in multiples of wall thickness) are shown in Figure 5. It can be observed from the figure that the axial strain decays rapidly with axial distance. For this particular example where the ratio of hoop to axial Young's moduli $E_1/E_2 = 2.705$, the axial strain at a distance of two thicknesses away from the impact point has a peak value that is less than one tenth the peak value on the distal surface at the impact point. At a distance of three thicknesses away from the centre, the axial strain becomes compressive. On the other hand, the hoop strain has a gradual decay, and still retains a peak value of more than one quarter of the initial magnitude at a distance of five thicknesses away from the impact point. This decay rate effect has important implications in the accuracy of experimental measurements of strain responses in such cylinders, especially as regards the gauge length of the strain gauges used and the precise location of the strain gauges in relation to the actual positions where strain measurements are required.

In their study, Christoforou and Swanson (1990) concluded that for an impact problem the response amplitude varies linearly with the velocity of impact. However, in their analysis the nonlinear local contact force term was neglected. This assumption may be valid in cases where the impactor has a large nose radius and there is no appreciable local contact deformation. However, it may not be appropriate in most cases, especially for impactors with small nose diameter colliding with thick shells, in which case the local indentation is

Table 1. Properties for a lamina layer of cylindrical shell*

Longitudinal Young's modulus, E_1 (GPa)	14.506
Transverse Young's modulus, E_2 (GPs)	5.362
Shear modulus, G_{12} (GPa)	2.509
Poisson's ratio, ν_{12}	0.231
Mass density, ρ (kg m^{-3})	1526
Cylinder internal diameter, a (mm)	216
Cylinder wall thickness, h (mm)	2.3
Total length, l (mm)	320
Winding angle relative to cylinder axis (outer layer to inner layer)	[90°,90°,90°,90°,90°,90°,90°,90°]

* Taken from Gong (1995).

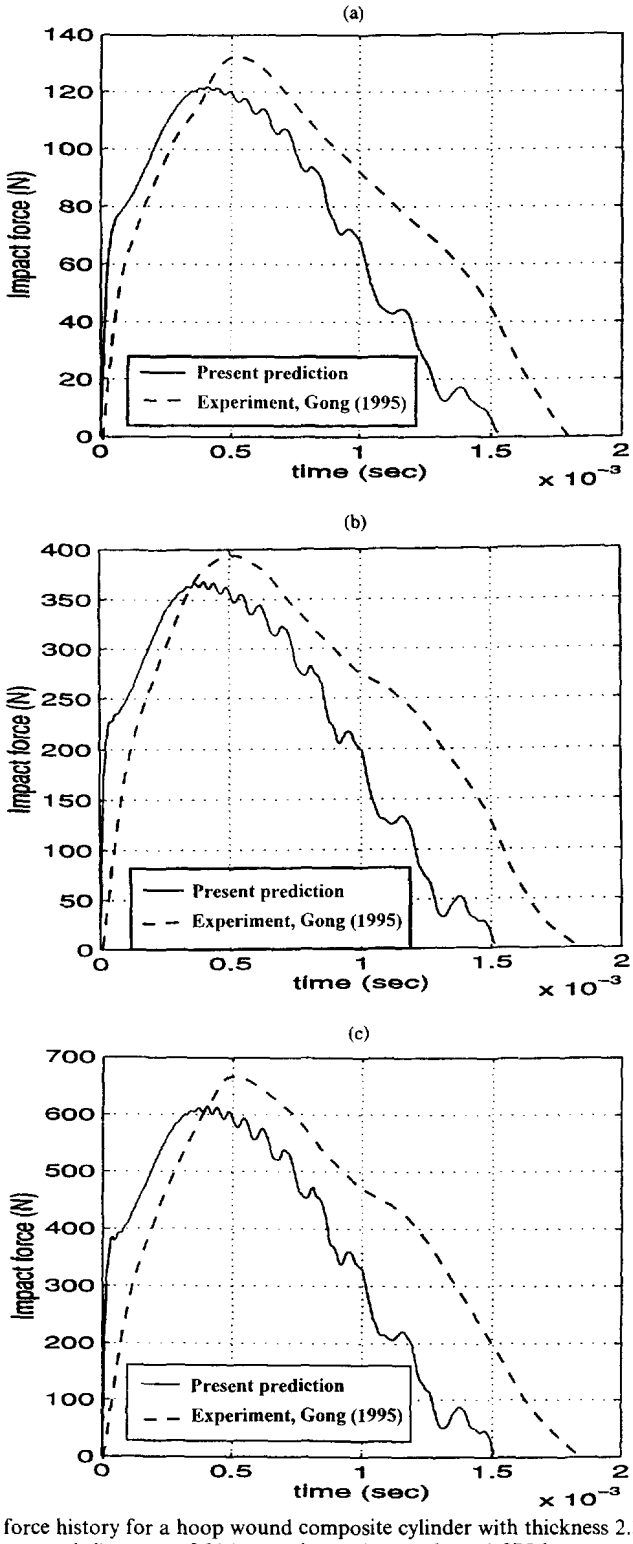

Fig. 2. Impact force history for a hoop wound composite cylinder with thickness 2.3 mm, effective length of 280 mm and diameter of 216 mm, due to impact by a 0.075 kg mass at a velocity of (a) 1 ms^{-1}, (b) 3 ms^{-1}, and (c) 5 ms^{-1}.

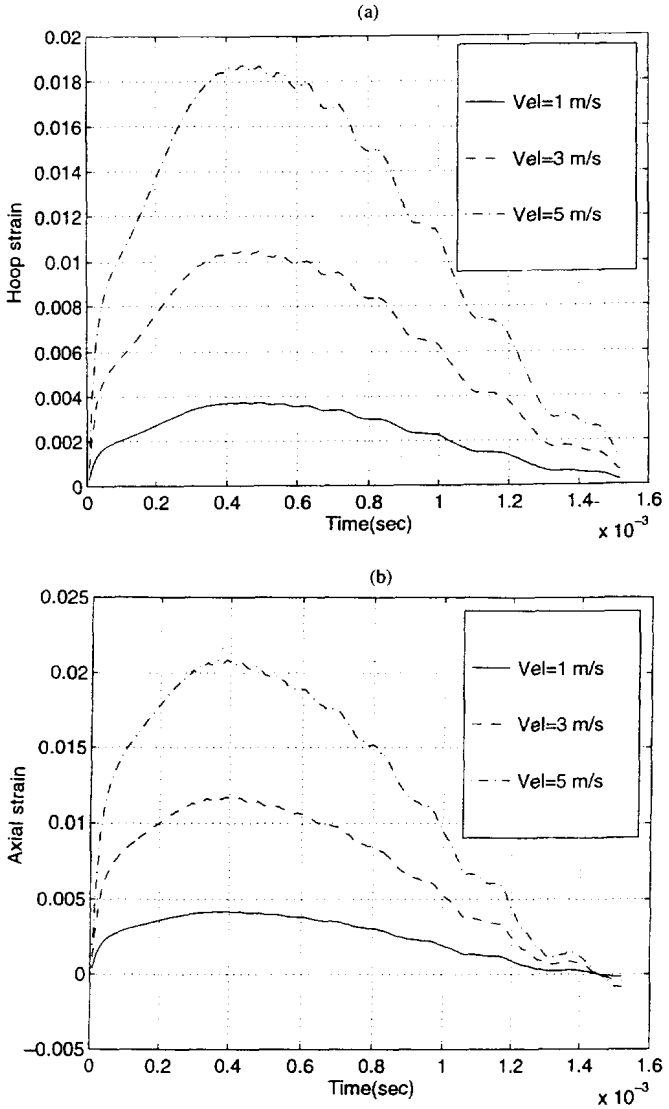

Fig. 3. Hoop strain histories (a), and axial strain histories (b), for a 2.3 mm thick hoop wound composite cylinder with effective length of 280 mm and diameter of 216 mm, due to impact by a 0.075 kg mass at velocities of 1 ms^{-1}, 3 ms^{-1} and 5 ms^{-1}.

not negligible in comparison with the global deflection. In order to ascertain whether the impact force actually varies linearly with the velocity of impact, the contact force history was calculated for impacts on a long composite pipe at velocities up to 100 ms^{-1}.

Figure 6 shows the plot of peak contact force against the velocity of impact for cylindrical shells with ratios of radius to thickness a/h of 50, 20 and 10. It can be observed that for all three plots there is a slight nonlinearity in the variation between contact force and velocity of impact. This is a consequence of the nonlinear Hertzian contact deformation term appearing in eqn (26). The importance of the contact force term cannot be over-emphasised considering the fact that in carbon fibre composite materials subjected to impact, large local stresses due to contact deformation have been known to cause both fibre damage and matrix cracking near the periphery of the contact region (Matemilola and Stronge, 1995).

The effect of the trapezoidal term z/a, which appear in the expressions for stress resultant and stress couple eqn (2), on the elastic solution can be studied by considering a cylinder with winding angle of $[90°, 0°, 90°, 0°, 90°, 0°]$ (outer to inner layer). This term affects the stress resultants and stress couples only if the layup is non-symmetric with respect

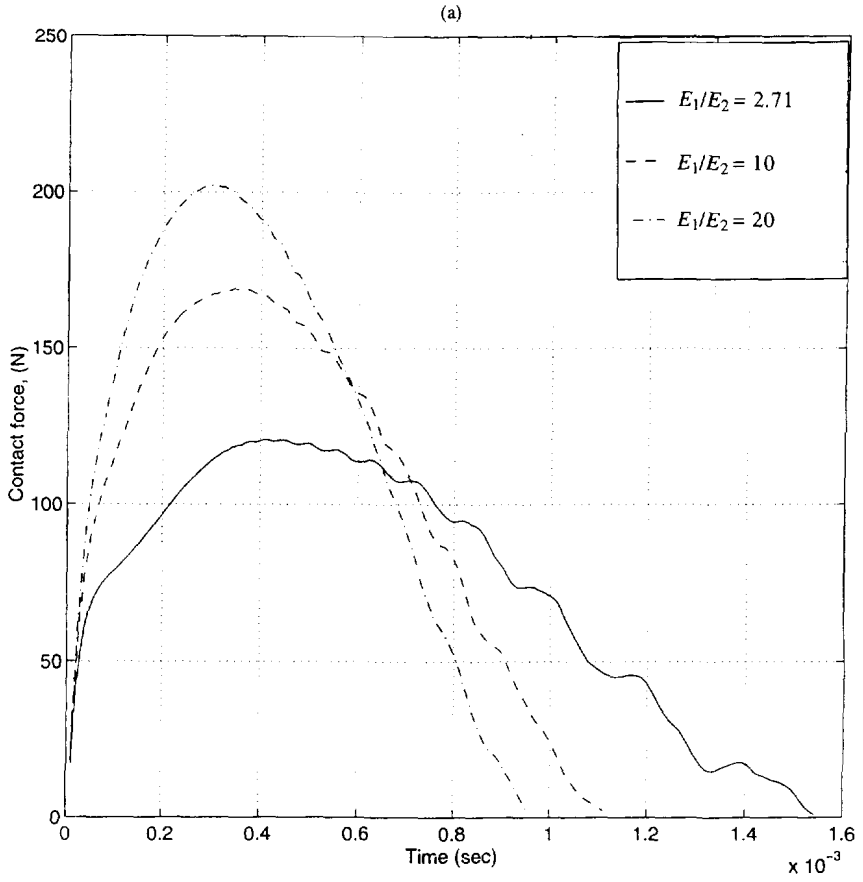

Fig. 4. The effect of ratio of orthotropy E_1/E_2 on the contact force (a), the hoop strain response (b), and the axial strain response (c) at the back surface of impact point, for a hoop wound composite cylinder due to impact by a 0.075 kg mass colliding at 1 ms^{-1}. Axial Young's modulus was kept constant at 5.362 GPa. (*Continued overleaf.*)

to the middle surface. The thick walled cylinder has a wall thickness of 5 mm, internal diameter of 50 mm and an effective length of 150 mm, and was struck by a 0.075 kg steel mass colliding at 1 ms^{-1}. The elastic properties (but not the layup) are given in Table 1. For this example problem, because the winding angle is non-symmetric with respect to the middle surface of the cylinder wall, the elastic stiffness coefficients $B_{ij} \neq 0$ and $E_{ij} \neq 0$. As such, the terms B_{ij}/a are no longer negligible in comparison with A_{ij} $(i,j = 1,2)$. Thus, the trapezoidal terms contribute to the resultant axial stress, as can be observed from the plots of the axial stress resultant.

Figure 7(a) shows that there is a decrease of 13% in the peak value of axial stress resultant in comparison with calculations which neglect the trapezoidal term. Figures 7(b) and (c) show that neglecting the trapezoidal term resulted in about 4% reduction in the peak axial strain, while the hoop strain response was practically unchanged. This is because for a cylindrical shell, the sides of an element taken from an axial section form a rectangle. Thus, the hoop stress resultant and the hoop stress couple are not affected by the trapezoidal term z/a, as can be observed from eqn (2). In considering the structural integrity of the cylinder for this example problem, the effect of the trapezoidal terms may be considered negligible. However, their importance cannot be overlooked if the cylinder had axial end loads, in which case the trapezoidal terms B_{ij}/a, D_{ij}/a and E_{ij}/a appearing in eqns (4) and (5) are directly involved in the calculations of the strain components. In this case, omitting these trapezoidal terms may lead to significant errors in the calculated strains and stresses.

6. CONCLUSIONS

An analytical procedure has been presented for calculating the impact response of simply supported orthotropic circular cylinders. Numerical examples for both thick and

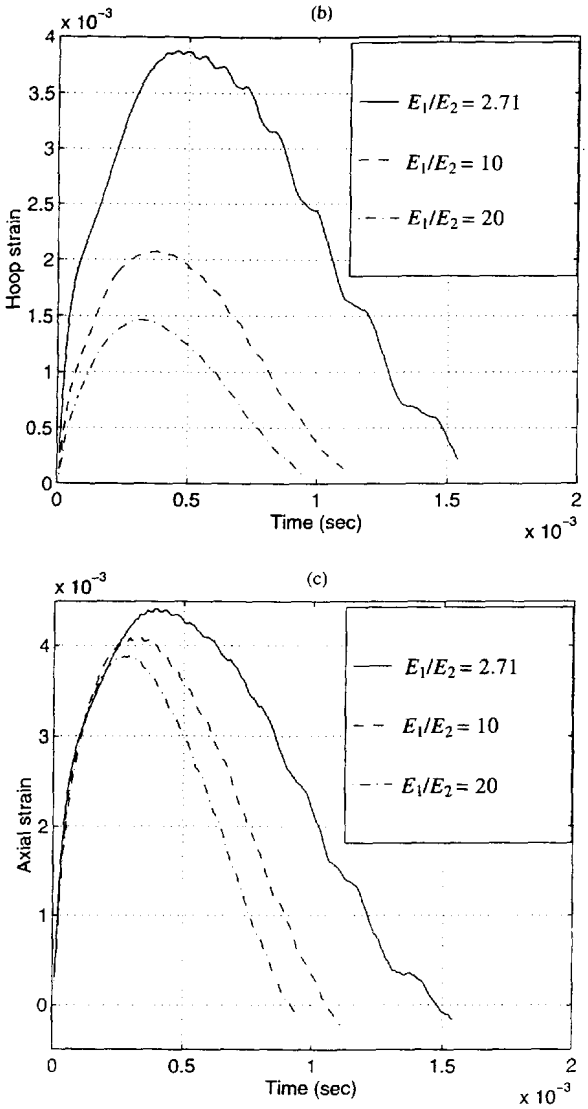

Fig. 4.—*Continued.*

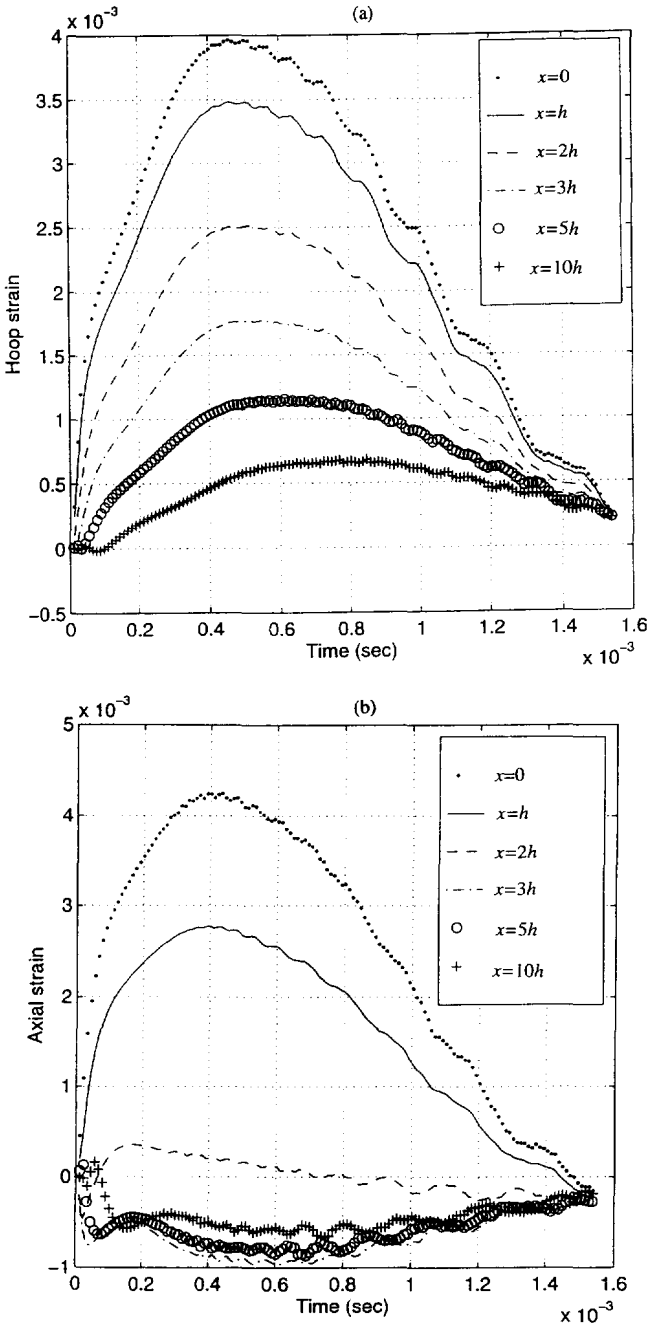

Fig. 5. The decay rate of hoop strain (a) and axial strain (b), at various locations along a generator of a 2.3 mm thick hoop wound composite cylinder with properties listed in Table 1.

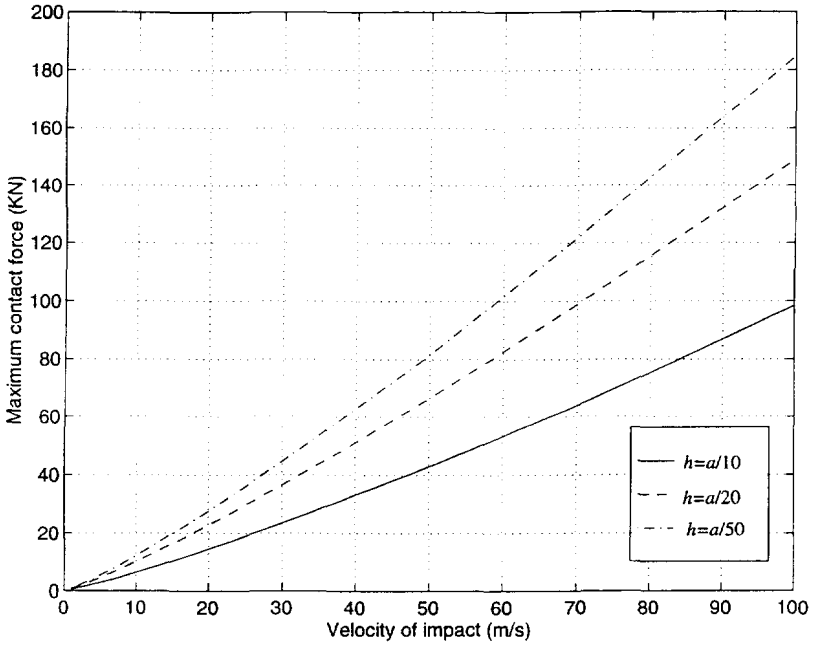

Fig. 6. Variation of the maximum contact force with the velocity of impact for impact on a hoop wound composite cylinder with an internal diameter of 216 mm, due to impact by a 0.075 kg mass, for ratio of cylinder diameter to wall thickness $a/h = 50$, $a/h = 20$, $a/h = 10$. The internal diameter of the cylinder was kept constant at 216 mm, while the thickness was varied.

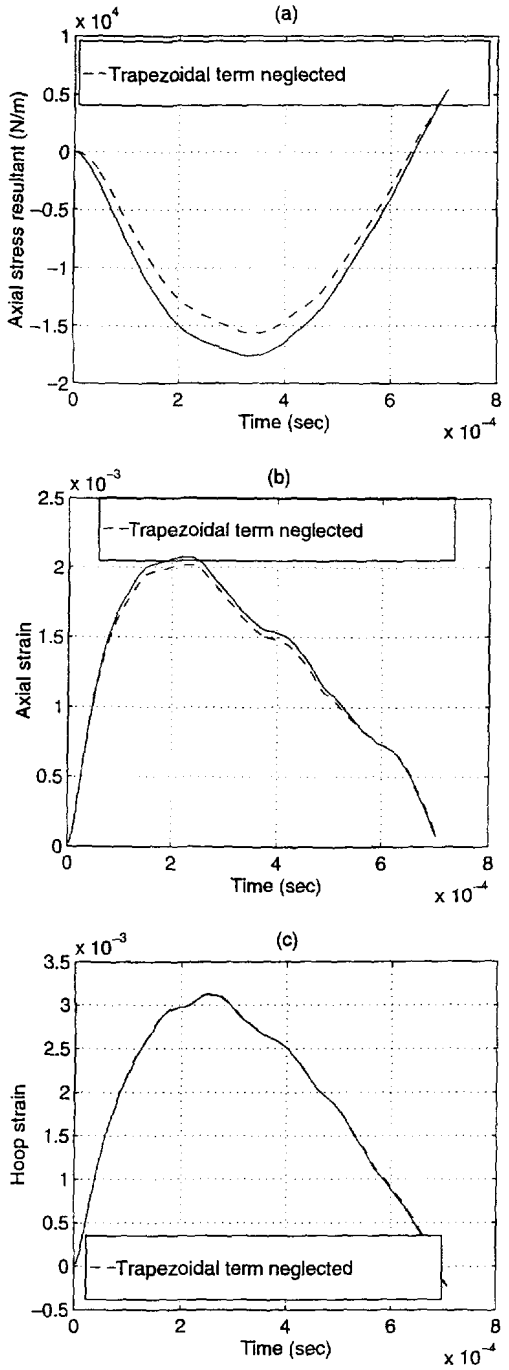

Fig. 7. The effect of trapezoidal terms B_{ij}/a, D_{ij}/a and E_{ij}/a on (a) maximum axial stress on the mid-section, (b) maximum axial strain and (c) maximum hoop strain response on the back surface at impact point. The 150 mm long composite cylinder has a wall thickness of 5 mm, internal diameter of 50 mm, and winding angle of $[90°, 0°, 90°, 0°, 90°, 0°]$ (outer layer to inner layer).

thin cylinders show that local contact deformation is important for an accurate solution of the impact response. By including the Hertzian contact deformation term in the analysis, the relationship between the contact force amplitude and the velocity of impact becomes nonlinear. Also, terms arising due to the trapezoidal shape of the cross-section of an element taken from the cylinder are important for accurate formulation of the elasticity problem. These terms significantly contribute to the accuracy of the calculated structural response of curved shells, especially for those with end loads. Numerical results show that the strain decreases slowly in the directions which have a relatively large modulus. This has important implications in the use of strain gauges in the experimental measurements of strain response of thin walled cylindrical shells.

REFERENCES

Agarwal, B. D. and Broutman, L. J. (1990) *Analysis and Performance of Fibre Composites*, second edition. John Wiley and Sons, Inc., New York.

Bert, C. W. and Birman, V. (1988) Parametric study of thick, orthotropic circular cylindrical shells. *Acta Mechanica* **71,** 61–76.

Bert, C. W. and Kumar, M. (1982) Vibration of cylindrical shells of bimodulus materials. *Journal of Sound and Vibration* **8,** 107–121.

Chandrashekhara, K. and Schroeder, T. (1995) Nonlinear impact analysis of laminated cylindrical and doubly curved shells. *Journal of Composite Materials* **29,** 2160–2179.

Christoforou, A. P. and Swanson, S. R. (1990) Analysis of simply supported orthotropic cylindrical shells subjected to lateral impact loads. *ASME Journal of Applied Mechanics* **57,** 376–382.

Flügge, W. (1973) *Stresses in Shells*, second edition. Springer-Verlag, Berlin, Heidelberg, New York.

Gerald, C. F. and Wheatley, P. O. (1989) *Applied Numerical Analysis*, fourth edition. Addison-Wesley Publishing Company, Menlo Park, CA.

Goldsmith, W. (1960) *Impact: The Theory and Physical Behaviour of Colliding Solids*. Edward Arnold (Publishers) Ltd., London.

Gong, S. W., Shim, V. P. W. and Toh, S. L. (1996) Central and non-central impact on orthotropic composite cylindrical shells. *AIAA Journal* (accepted).

Gong, S. W. (1995) A study of impact on composite laminated shells. PhD dissertation, National University of Singapore, pp. 125–145.

Lee, E. H. (1940) The impact of a mass striking a beam. *ASME Journal of Applied Mechanics* **62,** A129–138.

Matemilola, S. A. and Stronge, W. J. (1995) Impact micro-damage in resin transfer moulded (RTM) carbon fibre composite plates. In *Impact and Dynamic Fracture of Polymers and Composites*, ESIS 19 (eds J. G. Williams and A. Pavan). Mechanical Engineering Publications, London, pp. 371–381.

Qian, Y. and Swanson, S. R. (1990) A comparison of solution techniques for impact response of composite plates. *Composite Structures* **4,** 177–192.

Ramkumar, R. L. and Thakar, Y. R. (1987). Dynamics response of curved laminated plates subjected to low velocity impact. *ASME Journal of Engineering and Material Technology* **109,** 67–71.

Tan, T. M. and Sun, C. T. (1985) Use of statical indentation law in the impact analysis of laminated composite plates. *Journal of Composite Materials* **52,** 6–12.

Timoshenko, S. and Woinowsky-Krieger, S. (1987) *Theory of Plates and Shells*, second edition. McGraw-Hill Book Company, New York.

Yang, S. H. and Sun, C. T. (1982) Indentation law for composite laminates. *Composite materials: Testing and Design (Sixth Conference)*, ASTM STP 787, pp. 425–449.